ApJ 1997 submitted 4/21/97

X-RAY NOVAE, EVENT HORIZONS AND THE EXPONENTIAL METRIC

Stanley L. Robertson
(roberts@host1.swosu.edu)
Dept. of Physics, Southwestern Oklahoma State University, Weatherford, Oklahoma, 73096

Abstract

Recent models based on General Relativity attribute important spectral features of some accreting neutron stars to their surfaces and "gap accretion" while observations of x-ray novae indicate a surprising lack of distinguishing spectral characteristics between these neutron stars and black hole candidates. The shared spectral characteristics strongly suggest that both have surfaces without event horizons. Since many of the black hole candidates have masses known to be in excess of the 3 $M_\odot$ Schwarzschild limit for nuclear densities, the predicted existence of black holes may well be an error of General Relativity. The 3 $M_\odot$ limit can be removed by the Yilmaz modifications to General Relativity. The exponential metric of the Yilmaz theory has no adjustable parameters, passes the four classic weak-field tests, permits neutron stars of 10 $M_\odot$, and has no singularities, event horizons or black holes. General features of accretion disk and surface luminosities are compared here for gravitationally compact objects in the Yilmaz and Schwarzschild metrics. The gravitational fields, characteristic orbits and spectral characteristics of neutron stars in the two metrics are found to be very similar to 2 $M_\odot$. Above 2.0 $M_\odot$ in the Schwarzschild metric and 2.5 $M_\odot$ in the Yilmaz metric, neutron stars have radii smaller than that of the innermost marginally stable orbit. The spectral characteristics associated with the resulting "gap accretion" are precisely those exhibited by the black hole candidates. Massive stars in the Yilmaz metric are found to be capable of much more efficient conversion of accretion energy to x-ray luminosity than black holes. Additional binding energy may be released as other emissions from them. Future detailed comparisons of models with and without event horizons should finally decide the question of the existence of black holes. Contrary to common belief, mere possession of mass in excess of the Schwarzschild limit does not constitute proof that a compact object is a black hole.

Subject headings: Accretion, Black Hole Physics, Stars: neutron, Stars: novae, X-rays: stars

1. Introduction

X-ray novae appear in binary star systems in which one member is believed to be a neutron star (**NSB**) or, if suitably massive (or of appropriately variable x-ray luminosity), a black hole candidate (**BHC**). Since firm mass determinations can be made for some x-ray novae, they offer the best strong-field tests of gravity theories now available. According to General Relativity an object of nuclear density and more than 3 $M_\odot$ would exist as a black hole (Kalogera & Baym 1996, Friedman & Ipser 1987). At this time there are at least eight galactic x-ray sources known to exceed the 3 $M_\odot$ limit and perhaps twenty more candidates based on spectral similarities. Active galactic nuclei may also provide cases of masses that exceed a Schwarzschild mass limit. Although many astrophysicists have embraced the black hole theory, whether or not these compact objects are actually black holes is an open question that must ultimately be settled by observation and analysis.

A review (see below) of the spectral characteristics of x-ray novae strongly suggests that BHCs have surfaces rather than event horizons. If so, then the predicted existence of black holes would be a failure of a strong-field test by General Relativity. It will be shown that the 3 $M_\odot$ limit can be removed by adopting the Yilmaz modifications of General Relativity. The Yilmaz theory (Yilmaz 1958, 1971, 1992, 1994, 1995) has a strong metric similarity to General Relativity and passes the four classic weak-field tests. It has no adjustable parameters, no singularities and no event horizons (Alley 1995, Yilmaz 1994). It modifies General Relativity primarily by the explicit inclusion of the stress-energy of the gravitational field as a source of space-time curvature. With a true field stress-energy the Yilmaz theory possesses a field Lagrangian. It is a gauge-field theory and can be quantized (Yilmaz 1995). It permits local energy-momentum conservation and its metric tensor is formally exponential (Yilmaz 1992). Although gravitationally compact objects exist in the Yilmaz metric, they are not black holes. They are not subject to the "no-hair" theorem and they can retain intrinsic magnetic fields that may partially determine the properties of the inner accretion disk (van der Klis 1994). At nuclear densities they have well defined surfaces. There are only minor differences between the properties of neutron stars to ≈ 2 $M_\odot$ in the Yilmaz and Schwarzschild metrics, (see below) but in the Yilmaz exponential metric there is a smooth continuation of neutron star properties to masses beyond 10 $M_\odot$. This makes the Yilmaz metric an extremely useful tool for separating event horizon properties from those of active surfaces. At the very least, it offers a chance to prove by negation what has eluded direct demonstration within the framework of general relativity, but it is also possible that a flawed (Alley 1995) General Relativity will stand corrected. In addition to the strong-field black hole predictions considered here, Alley (Alley 1995) and Yilmaz (Yilmaz 1994) have shown that General Relativity fails to yield the static limit gravitational attraction of two small slabs of mass arranged as a Cavendish balance.

2. X-Ray Novae

X-ray novae display a rich mix of spectral characteristics. Maximum luminosities during major flares are often $\approx 10^6$ - 10^8 times quiescent luminosities. Maximum luminosities are often near the Eddington limit, which is about 2 x 10^{38} erg/s for a 1.4 $M_\odot$ neutron

star. Complex changes of luminosities in x-rays (0.1-4.0 keV), hard x-rays (4-20 keV) and hard tails, (20-200 keV) occur during flares. Hard tail luminosity with an inverse power law dependence on photon energy is observed during the initial rise of luminosity and then may largely die away for a time before becoming prominent again during the subsequent approach to quiescence. Hard tails have not been seen at luminosities approaching the Eddington limit. An "ultrasoft" feature (White & Marshall 1984) with a general brehmsstrahlung shape and a peak near 1 - 2 kev is often seen at high luminosities. BHCs often simultaneously display hard tails and ultrasoft peaks. Spectral state switching occurs between soft "high" luminosity states and harder "low" states characterized by power law spectral features. This typically occurs for luminosities of 10% - 30% of the Eddington limit, often near $\approx 10^{37}$ - 10^{38} erg/s. Arrests of decline or luminosity increases are sometimes seen during the transition (Ebisawa et al. 1994). Low frequency, $\approx$ 5 - 6 Hz, quasi-periodic oscillations (QPOs) often appear in the hard x-rays of suitably "high" states (Miyamoto, Kimura & Kitamoto 1991, Makishima et al. 1986). Flickering (large amplitude $\approx 10^{-3}$ - 10 s luminosity variation) occurs in the power law components (Balucinska-Church et al. 1997, Tennant, Fabian & Shafer 1986, Stella et al. 1985) and the variations of hard power law components and soft x-rays are often uncorrelated (Pan et al. 1995) or anti-correlated. All of these features, some of which were once thought to be black hole signatures, have been observed in both BHCs and NSBs (e.g., see Singh et al. 1994, Barret, et al. 1992, Churazov, et al. 1995, Stella et al. 1985). Cir X-1 is perhaps the most infamous of several neutron stars which were once respectable BHCs (Sunyaev and Trümper 1979, Stella et al, 1985), until their candidacies were ended without mass determination by observations of bursts (Tennant, Fabian and Shafer) or pulses. GX 339-4 may soon depart the BHC list after observations of millisecond pulsations (Imamura, Steiman-Cameron & Middletich 1987) and a mass estimate of 2.5 $M_\odot$.

The similarities of NSB and BHC behavior have been recently noted by others (Walker 1992, van der Klis 1994, Barret, McClintock and Grindlay 1996, Tanaka & Shibazaki 1996). Barret et al. conclude that the presence of a hard x-ray tail at overall luminosity above 10^{37} erg/s is the only spectral feature that distinguishes BHCs from NSBs. Tanaka and Shibazaki (Tanaka & Shibazaki 1996) state that there are no characteristic differences in quiescent x-ray spectra of NSBs and BHCs. They further state that the remarkably similar ratios of x-ray to optical luminosities between NSBs and BHCs implies a common origin of the soft x-rays in quiescence for both systems. Walker (Walker 1992) concluded that BHCs are simply massive neutron stars, though he gave no explanation of how they might exceed the 3 $M_\odot$ limit.

Despite the profound differences between hard surfaces and event horizons, the only known black hole characteristics shown by BHCs are absence of bursts or pulses and mass, when known, in excess of 3 $M_\odot$. On the other hand, it is very clear from recent developments in gap accretion models that are based on general relativity (Fortner, Lamb and Miller 1988, Hanawa 1991, Kluzniak and Wilson 1991, Walker 1992) that several key spectral features of some NSBs arise from the stellar surface and boundary layer. Observations of the same phenomena in BHCs then strongly suggests that they also have surfaces. These phenomena include flickering, production of hard tails, hard-

ening of quiescent spectra, spectral state switching and 6 Hz QPOs. The first three of these are based on the strong-field phenomena of marginally stable orbits and gap accretion which have no Newtonian physics counterparts. If a star radius is smaller than that of the innermost marginally stable orbit, then accreting matter which progresses to this level will eventually fall onto the surface with a radial velocity component which is a sensible fraction of the speed of light. The supersonic radial flow separates and decouples the inner accretion disk from the boundary layer on the star (Kluzniak and Wilson 1991). Hard x-rays can be produced by Comptonization of soft photons from the star atmosphere by the bulk accretion flow (Hanawa 1991, Kluzniak and Wilson 1991, Walker 1992). Multiple scatterings of photons within the boundary layer on the star and between the boundary layer and the inner ring of the accretion disk can produce photons above 200 keV in the rest frame of the star surface. At low luminosity levels gap accretion is marked by strong aperiodic variability with radiation overwhelmingly dominating the interaction between the surface and the disk (Walker 1992). Despite the fact that both hard x-ray production and flickering were once considered to be black hole signatures, how they might be produced by black holes is still unknown (Joss & Rappaport 1984, Kusunose, Minishige & Yamada 1996).

3. The Yilmaz Metric

The static limit of curved space-time metrics corresponds to situations dominated by objects moving at speeds which are only a small fraction of the speed of light. While this is clearly inappropriate for the small amounts of accreting matter, the metric of space-time in the vicinity of neutron stars is dominated by the gravity of the star which is considered here to be a static object. The static limit interval in the Yilmaz exponential metric is:

$$ds^2 \;=\; g(r)c^2dt^2 \;-\; (dr^2 \;+r^2d\theta^2 + r^2\sin^2\theta d\phi^2)/g(r) \tag{1}$$

where:

$$g(r) \;=\; \exp(-2u(r)) \tag{2}$$

and $c^2u(r)$ is the gravitational potential. In the Schwarzschild metric:

$$ds^2 \;=\; g(r)c^2dt^2 \;-\; dr^2/g(r) \;-\; r^2d\theta^2 \;-\; r^2\sin^2\theta d\phi^2 \tag{3}$$

and:

$$g(r) \;=\; 1 \;-\; 2u(r) \tag{4}$$

It can be easily shown that the exponential metric follows from special relativity and the principle of equivalence applied to frames co-moving with an accelerated particle (e.g., see Rindler 1969). That this metric does not satisfy the field equations of General Relativity was one of the motivations for the earliest version of the Yilmaz theory (Yilmaz 1958). It is noteworthy that the the exponential metric is merely rescaled by addition of an arbitrary constant to the potential whereas the Schwarzschild metric depends on an absolute potential. With the conventional choice of zero potential at

infinity, however, the two metrics are the same to first order in u(r) and this is sufficient to insure that they give the same results in the four classic weak-field tests of General Relativity. An event horizon exists for $u(R_s) = 1/2$ in the Schwarzschild metric. Gravitational redshift of radiation observed distantly is given by (Rindler, 1969):

$$z \;=\; \exp(u(r)) \;-\; 1 \tag{5}$$

and in the Schwarzschild metric:

$$z \;=\; \frac{1}{\sqrt{1 \;-\; 2u(r)}} \;-\; 1 \tag{6}$$

Either a star atmosphere or an innermost marginally stable orbit marks the inner boundary of the accretion disk. When the marginally stable orbit lies outside the radius, R, of the star (or event horizon, R_s for a black hole) gap accretion and hard photon production occurs. At moderate accretion rates it is unlikely that appreciable x-ray luminosity might be generated within the gap itself. The inward flow quickly becomes supersonic, decoupled from the disk, and then near-relativistic for neutron stars with $u(R) \approx 1/4$ ($\approx 3\ M_\odot$, see appendix). For more massive objects in the Yilmaz metric the radial speed becomes strongly relativistic near the surface. For black holes the radial speed would reach the speed of light at the event horizon. The rapid decrease of density as mass falls into the gap would render it optically thin and strongly suppress radiation from the gap. Realistically, magnetic field "propeller effects" might even push the inner disk radius to larger values; except for black holes.

An accreting particle starts from a large radial distance, with essentially zero momentum and $u(r) \approx 0$. Its energy is $E = m_0c^2$. It is assumed here that it will arrive in a circular marginally stable orbit at r_{ms} with radial momentum component $p_r = 0$, having transferred some portion of its energy to radiation. At r_{ms}, in the Yilmaz metric, $u(r_{ms}) = 0.191$ and the energy of an orbiting particle is $E = 0.945m_0c^2$ (see appendix). The maximum energy which a particle can transfer to radiation from the disk would therefore be $(1 - .945)m_0c^2 = 0.055m_0c^2$. Whether this amount can be radiated and what portion would be hard photons depends in part upon whether or not the disk extends to the star surface. In the event that r_{ms} lies within the star surface, hard photon production is suppressed. In this case the boundary layer is defined to begin where the average radial velocity of accreting particles is zero. The particle energy at this location can be shown (see appendix) to be $E=m_0c^2 \exp(-u)\{(1 - u)/(1 - 2u)\}^{1/2}$. Thus, in the Yilmaz metric the maximum fraction of accretion mass energy which can be observed as radiation from the disk is:

$$f_d \;=\; 1 \;-\; \exp(-u)\sqrt{\frac{1-u}{1-2u}} \tag{7}$$

limited to $u < 0.191$.

For the Schwarzschild metric the maximum fraction of accretion mass energy which can be radiated from the disk, limited to $u < 1/6$ and $0.057m_0c^2$, is:

$$f_d \;=\; 1 \;-\; \frac{1 \;-\; 2u}{\sqrt{1 \;-\; 3u}} \tag{8}$$

With the innermost marginally stable orbit as the inner disk boundary, disk mechanics and disk luminosity should be essentially indistinguishable and mass independent above $\approx$ 2 $M_\odot$ for the two metrics. If not for the surface emissions of neutron stars, the similarities of NSBs and BHCs would be theoretically assured, though likely very different from what is actually observed.

For neutron stars there is additional energy dissipated in the boundary layer as accreting particles are brought to rest. Evaluating the energy-momentum four-vector for zero momentum shows the energy of a particle at rest on the star to be $E = m_0c^2\sqrt{g(R)}$. Thus the total accretion energy, external to the star, which may be directly radiated to distant observers is m_0c^2 (1 - $\sqrt{g(R)}$). The fraction radiated from the star surface itself (neglecting fusion, which can be considered as part of the binding to the star) would be:

$$f_s \;=\; 1 \;-\; \sqrt{g(R)} \;-\; f_d \tag{9}$$

In the strong-field cases to be considered here, over half of the energy release exterior to the star occurs within 3R and $\approx$ 90% from within 10R.

4. Compact Objects

To go beyond these generalities some model of a compact object is needed. In this case we will consider an object of *constant intrinsic local density*, however, the appropriate equations will be set up for a more general case. Consider a spherically symmetric density distribution $\rho_0 h(r<R)$ with ρ_0 a constant and h(r) a distribution function for density. The condition h(0) = 1 is imposed without loss of generality, and all mass is confined within radius R relative to an external observer. In this model, the proper density, $\rho(r)g(r)$ is assumed to be given by $\rho_0 h(r)$. Thus it will be assumed that $\rho(r) = \rho_0 h(r)/g(r)$. As shown by Clapp (Clapp 1973), u(r) can be constructed by adding the potentials of successive shells of matter. Inside each shell the contribution to u(r) is constant and outside it declines as 1/r. For a general radius r, with r < R, contributions to the potential must be separated into those arising from shells of radius r' inside r and those from shells of radius r' outside r. The gravitational mass within each shell is $4\pi r'^2 \rho_0 h(r')dr'/g(r')$. (For the free baryon mass substitute $g(r')^{3/2}$.) The central potential u(0) is obtained by dividing each shell mass increment by r' and integrating out to R. Subtracting u(0) from u(r<R) leads to Clapp's integral equation:

$$u(r < R) \;-\; u(0) \;=\; \frac{-4\pi G{\rho_0}^2}{c} \int_0^r dr'\; h(r')(r' \;-\; r'^2/r)\; /g(r') \tag{10}$$

It can be shown that this equation is a solution of the field equations of either gravitational theory by substitution of the appropriate g(r) and other metric components into the field equations and solving the G_{tt} differential equation for u(r). By expressing u(r<R) and u(0) in terms of g(r) and g(0) and incorporating g(0) into a scale factor for lengths, the integral can be recast in the dimensionless form:

$$y(x) \;=\; -\,2\int_0^x f(x')h(x')(x' \;-\; x'^{\,2}/x)dx' \tag{11}$$

where x = r/($r_0 g(0)^{N/2}$), $r_0 = c/\sqrt{4\pi G\rho_0}$, f(r) = g(0)/g(r), N = 1 in the Yilmaz metric and N = 2 in the Schwarzschild metric. Thus these collapsed objects can be described with the aid of the characteristic radius, r_0, and a characteristic mass, $M_0 = c^2 r_0/G$. In the exponential metric:

$$y(x) \;=\; \ln(f(x)) \tag{12}$$

and in the Schwarzschild metric:

$$y(x) \;=\; 1 \;-\; 1/f(x) \tag{13}$$

After substituting the appropriate left member, Eq. 11 can be numerically solved for f(x) by an iterative relaxation method starting from f(x) = 1 for x < 1 and an asymptotic value for x > 1. Asymptotic solutions for the constant intrinsic density model, for which h(r) = 1 are $f(x) = x^{-2}$, x^{-1}, for the Yilmaz and Schwarzschild metrics, respectively. Physical quantities such as gravitational mass m_g, equivalent free baryon mass,m_b, distantly observed red shift of surface radiations, z and radius, R can be expressed in terms of certain integrals over f(x). Following Clapp (Clapp 1973), these are:

$$F_1(x) \;=\; \int_0^x h(x')f(x')x'dx' \tag{14}$$

$$F_2(x) \;=\; \frac{1}{x}\int_0^x h(x')f(x')x'^{\,2}dx' \tag{15}$$

$$F_3(x) \;=\; \frac{1}{x}\int_0^x f(x')^{3/2}x'^{\,2}h(x')dx' \tag{16}$$

In the exponential metric there follows:

$$m_g \;=\; M_0 x\; F_2(x)\; \exp(-F_1(x)) \tag{17}$$

$$m_b \;=\; M_0 x\; F_3(x) \tag{18}$$

$$R \;=\; r_0 x\; \exp(-F_1(x)) \tag{19}$$

$$u(0) \;=\; F_1(x) \tag{20}$$

$$u(R) \;=\; F_2(x) \tag{21}$$

In the Schwarzschild metric the same quantities are given by:

$$m_g \;=\; M_0\frac{x\; F_2(x)}{(1\;+\;2F_1(x))^2} \tag{22}$$

$$m_b \;=\; M_0\frac{x\; F_3(x)}{(1\;+\;2F_1(x))^{3/2}} \tag{23}$$

$$R \;=\; r_0\frac{x}{(1+2F_1(x))} \tag{24}$$

$$u(0) \;=\; \frac{F_1(x)}{1\;+\;2F_1(x)} \tag{25}$$

$$u(R) \;=\; \frac{F_2(x)}{1 \;+\; 2F_1(x)} \tag{26}$$

Numerical solutions of Eq. 11 and the appropriate integrals for the case h(r) = 1 were used to generate the data of Table 1 and Table 2. Plots of mass, radius and redshift for surface emissions are shown in Figures 1 and 2. Choosing h(r) = 1 forces the object to be of *constant local intrinsic density*. To an external observer, there would be substantial variations of density, but locally everything would seem entirely normal. Such is life in radically curved space-time. Simple extensions of this approach to an Oppenheimer - Volkoff method for the determination of ρ_0 and h(r) are possible, as well as exponential atmosphere models of active galactic nuclei, but the essential differences between black holes, neutron stars and nuclear-density compact objects in the exponential metric are clearly revealed by this simple model.

With a suitable choice of ρ_0, the features shown in Figures 1 and 2 can be evaluated for neutron stars. The choice of density ρ(R) $\approx$ 2 x 10^{14} gm/cm^3, as a typical nuclear density in the outer layers (below the crust) of a neutron star and u(R) $\approx 1/4$ (See Table 2) for the most massive stars in the Schwarzschild metric leads to $\rho_0 = 10^{14}$ gm/cm^3, r_0 = 32.8 km and M_0 = 22.1 $M_\odot$. For the Schwarzschild metric the solutions truncate with a core collapse at u(0) = 1/2 for a gravitational mass of 2.8 $M_\odot$. This is the maximum static neutron star mass recently reaffirmed by Kalogera and Baym (Kalogera & Baym 1996). Its radius would be 16 km and the mean density for a distant observer would be 3x10^{14} gm/cm^3. The mass-radius characteristics in this model are similar to those found for a very stiff neutron equation of state. (Unless otherwise noted, "mass" will refer to gravitational mass.) In the exponential metric there is a maximum mass of about 10.5 $M_\odot$ but no black hole termination. A maximum radius occurs for a mass of 6 $M_\odot$. For masses above 1.0 $M_\odot$ there is so little variation of radius in either metric that it could be regarded as constant to a good approximation. Clearly, we could choose a different intrinsic density and obtain somewhat different maximum masses and radii for both metrics, but these results are consistent with the best current estimates of mass limits and they should suffice for a general comparison of spectral properties. Independent of the choice of ρ_0, the most massive one third of the neutron stars in the Swarzschild metric would have u(R) $> 1/6$ and have radii small enough for them to display gap accretion. Since many NSBs do not display gap accretion signatures, raising ρ_0 and lowering the mass at which gap accretion would occur does not seem to be plausible. On the other hand, lowering the choice for ρ_0 very much would be inconsistent with our knowledge of nuclear density. For rigidly rotating stars, mass limits and maximum radii of both metrics would likely be extended by about 25% (Friedman & Ipser 1987). For differentially rotating stars or oblate stars, the present model fails and there may be no limiting gravitational mass for the exponential metric.

5. Surface and Accretion Disk Luminosities

The innermost marginally stable circular orbit occurs for $r_{\rm ms} = 4u(R)R/(3-\sqrt{5})$ in the Yilmaz metric (see appendix). Thus for u(R) $> .191$ (i.e., for $m_g > 2.5$ $M_\odot$), the disk terminates above the surface and gap accretion occurs. In the Schwarzschild metric,

gap accretion occurs for $u(r_{ms}) > 1/6$ (for $m_g > 2.0\ M_\odot$). It can be ascertained by calculation of the Schwarzschild radius for softer neutron equations of state (Kalogera and Baym 1996) that gap accretion must always occur in the Schwarzschild metric for about the upper third of the allowed range of masses. Conversion efficiencies, f_d and $f_d + f_s$ calculated using Eqs 7, 8 and 9 are shown in Fig. 3. It is apparent from Fig. 3 that a massive Yilmaz object would be about twelve times as efficient as a black hole as the overall conversion fraction, $f_d + f_s$, reaches 70%. Accretion disks for black holes are no more efficient than those of Schwarzschild neutron stars of more than 2.0 $M_\odot$ and black holes would be limited to just the disk efficiency of about 5.7%.

A profound effect of the neutron star surface is implied by Fig 3. Up to about $\approx 1.4\ M_\odot$, the luminosity is fairly evenly divided between disk and surface, but for the largest masses in the Schwarzschild metric up to 80% of the luminosity must arise from the star surface. In the Yilmaz metric as much as 90% of the luminosity would originate from the star surface. It is probable, however, that much of it would be reprocessed by beaming into the disk.

Although it seems to be widely assumed that soft spectral features arise almost entirely from the accretion disk, it has been noted that the necessary mass accretion rates would be too high for this to be the case (Czerny et al. 1986, White, Stella & Parmar 1988). Thus the strong surface contributions should consist of both hard and soft radiations.

i) Hard emissions and quenching:

The nature of surface emissions is strongly dependent on the size and optical depth of the boundary layer. If too optically thin, hard photons are produced with only low efficiency. If too thick, then it thermalizes x-rays. Hanawa (Hanawa 1991) showed that the boundary layer of a neutron star ($< 3\ M_\odot$) could remain optically thin enough to efficiently produce very hard x-ray emissions to luminosities of $\approx 10^{37}$ erg/s. He also noted that the optical thickness of the boundary layer is inversely proportional to the proper gravitational acceleration at the surface. Since this acceleration is in turn roughly proportional to the mass of the star, (see Table 1) it follows that the boundary layer could remain optically thin and produce very hard photons to about 10^{38} erg/s for a 10 $M_\odot$ neutron star. Thus the sole distinction between BHCs and NSBs (Barret, McClintock and Grindlay 1996) is seen to be straightforwardly mass dependent in the Yilmaz metric and unrelated to event horizons. In addition, the observed quenching of hard x-rays at luminosity levels approaching the Eddington limit can be attributed to the increased optical and physical thickness and areal extent of the boundary layer. The "high - low" switching of both BHCs and NSBs is very likely caused by opacity variations of the boundary layer. In the switching regime, hard and soft x-ray emissions would be anti-correlated.

The radial velocity of matter reaching the boundary layer becomes more strongly relativistic as mass increases and the gap widens. Therefore, as observed, more massive objects are capable of producing much harder x-rays from harder shear and impact at the surface.

ii) Quasi-periodic oscillations (QPOs):

At relatively high luminosity levels, strong $\approx$ 5 - 6 Hz QPOs often appear in the hard x-rays of suitably "high" states of both BHCs and NSBs (Miyamoto, Kimura & Kitamoto 1991, Makishima et al. 1986). These have been explained as accretion disk flow oscillations driven by surface radiations from neutron stars (Fortner, Lamb & Miller 1989). It is not known how they could be produced by black holes.

At high accretion rates, but somewhat below those associated with 6 Hz QPOs, radiation pressure in the boundary layer and radiation torques on the inner disk might first cause the accretion gap to close. This would be marked by a reduction of hard emissions. Biehle and Blandford (Biehle and Blandford 1993) have suggested that intermittent closure of the gap might explain the behavior of the Rapid Burster. They also propose that gap closure marks the apex transition from the "horizontal branch" to the "normal branch" of z-source neutron stars. Van der Klis (1994) attributes the same phenomena to magnetospheric effects. In neither case is a black hole involved, however, there is a strong similarity between the normal branch z-sources and the "high" states of BHCs.

iii)Flickering:

At low accretion rates, the inner disk is completely exposed to the radiations from the boundary layer. Bulk Comptonization occurs in both the boundary layer and in the inner rings of the accretion disk. In this case, Walker (Walker 1992) pointed out that the total system luminosity is dominated by the power arising from bulk Comptonization in multiple photon scatterings between the disk and the boundary layer. Even though the boundary layer alone inefficiently produces hard x-rays, the quiescent energy spectrum is dominated by the power-law emissions. Since the power is derived from the accretion, radiation stresses control the dynamics of the disk. The disk/star/radiation field is a completely nonlinear system with positive feedback. This very likely accounts for the flickering exhibited by quiescent BHCs.

The shortest time scales associated with flickering would correspond to the gap transit time for inner disk particles perturbed by photons from the star. For a rough estimate, this would be some fraction one star radius; $\approx$ 16 km at $\approx 10^9$ cm/s, or $\approx 10^{-4}$ s. One imagines a shot beginning with random photons perturbing disk particles followed by the positive feedback of additional photons released as these particles fall on the star and ending when the inner disk is at least partially depleted to a considerable radial distance. The longest time scales of $\approx$ 1 s should correspond to transit times associated with the radius of depletion. A further consequence of perturbed particles falling from greater radial distances is that the radial components of velocity can become strongly relativistic. The higher radial velocity would cause the emission of harder x-rays and explain the observed spectral hardening (Miyamoto et al. 1992) as shots progress. Greater time delays for the hard photons produced (Miyamoto et al. 1988) would also result from the infall from larger radial distances and the multiple scatterings involved in their production.

iv) Quiescent soft radiation:

Power law components dominate the emissions of both BHCs and NSBs in quiescence, but there are also "excess" soft emissions. These typically have temperatures of 0.1 - 0.2 keV and correspond to radiating areas of 10 - 100 km^2 (Tanaka and Shibazaki 1996). The temperature is too high and the radiating area too small to correspond to emissions from the inner ring of the disk. The obvious explanation, suggested by Verbunt et al., (Verbunt et al. 1994) is that they arise primarily from a boundary layer belt or polar cap on a neutron star. This suggestion was apparently rejected because black holes cannot have surfaces (Tanaka and Shibazaki 1996), however, no other plausible explanation has been offered.

6. Internal Processes

After accreted matter reaches the surface there is still energy to be produced by fusion and a need for additional gravitational binding energy to be released by the star. In order to properly account for all of the energy available, one needs to consider the difference between free baryon mass and mass bound gravitationally within the star. The total gravitational energy release as rest mass Δm_b falls from a large distance and becomes bound in the star would be $c^2(\Delta m_b - \Delta m_g)$, or $c^2 \Delta m_b(1 - dm_g/dm_b)$. The term in parentheses is the maximum possible fraction of accreted rest mass to be converted to radiations seen by a distant observer. It is plotted in Figure 4 as the gravitational binding fraction of the object. For a neutron star in the Schwarzschild metric, it actually diverges shortly after it reaches 1.0 just below 2.8 $M_\odot$. At this point the constant intrinsic density model may fail in the Schwarzschild metric, but it doesn't matter. The addition of more mass simply causes a core collapse, though it may be possible that some of the binding energy would escape through neutrino emission, pair production and gravitational radiation. The diverging binding fraction for constant intrinsic density shows that it is fundamentally wrong to consider the core collapse to be due to a pressure increase. It is the increase of central potential as exterior shells of mass are added that causes a metric collapse. It is a strange and unphysical result depending on an absolute potential; a phenomenon found nowhere else in physics.

In the Yilmaz metric, there is no discontinuity of binding fraction but after trapped baryons reach maximum star gravitational mass, the infall of more matter can trigger the release of additional energy as the star becomes more tightly bound. The more massive neutron stars permitted in either metric swallow baryons but essentially expel their mass equivalents. Surface and external x-ray and optical emissions account for almost none of the binding fraction for very small mass neutron stars, but the external contributions quickly rise to about 50% of the binding fraction as mass increases from zero to about 1.0 $M_\odot$. They decrease to about 40% near maximum mass in the Schwarzschild metric and then quickly become comparatively insignificant as the binding fraction diverges. In the Yilmaz metric, external emissions increase to about 2/3 of the binding fraction by the time 10 $M_\odot$ is reached. Thus substantial additional radiations of some kind should be seen from neutron stars in either metric. It is possible that this energy would appear as copious neutrino or pair plasma emissions, or gravitational radiation. It might possibly be transiently accumulated within the star and released later.

Perhaps this is the source of the delayed transient super-Eddington emissions needed to drive the radio lobes of the BHC, GRS 1915+105 (Mirabel & Rodriguez 1994, Sazanov et al. 1994). Exactly how a black hole might produce power in excess of the Eddington limit is an interesting question. To do so after a two-week delay is likely beyond realistic expectation for a black hole.

Finally, if we consider the possible beginnings of x-ray novae in supernovae detonations, it would seem that a solid core object supporting shock waves and not seriously limited in the number of baryons remaining in its core would be far more likely to drive a detonation than one which implodes.

7. Discussion

The observed spectral features of NSBs are affected by many complex factors such as viewing inclination angle, thicknesses and opacities of the accretion disk and boundary layer, areal extent of the boundary layer, magnetic field strength, stabilization or destabilization of the inner disk by radiation, etc. The simple circumstance of observing at small inclination angle might prevent one from detecting much direct hard radiation from the boundary layer belt. Nevertheless, the properties of NSBs are strongly affected by the presence of a surface. The more massive ones **in either metric** must also display the signatures of gap accretion and surface/disk/radiation interactions. To recapitulate, these are hard photon production, flickering, progressive spectral hardening of shots, hard time delays, 6 Hz QPOs, high-low switching and small area soft excess emissions in quiescence. It is difficult to see how all of these features that are also observed in BHCs could arise in a completely different way from just a gently sheared disk and no surface. Given sufficient mass to produce gap accretion, the disk properties outside the marginally stable orbit are essentially independent of the central mass. It seems impossible that there could be disk processes so strongly mass dependent that they would not operate for gap-accreting stars below 3 $M_\odot$, which have no need of a second set of mechanisms. The properties of BHCs seem to simply be inconsistent with event horizons. If not for the historical development of the concept of an event horizon, it would seem quite absurd to hypothesize the disappearance of a surface as an explanation of the differences between low mass and high mass x-ray sources.

Difficulties arise when one tries to model BHCs without surfaces, especially if the disk model is then applied to NSBs. Geometrically thin, but optically thick disk models are usually used to describe the soft features of the disk over a broad range of luminosity. In these models the gas radiates energy immediately as it is derived from viscous dissipation of gravitational potential energy. The thin disk model has often been embellished in ad hoc fashion (e.g., Sunyaev and Trümper 1979) to explain the hard x-rays of BHCs. Usually, the hard x-rays are assumed to be generated by Compton up-scattering of soft photons from the disk. The scattering is assumed to arise from a hot coronal electron cloud with electron temperature, $T_e \approx$ 20-50 keV, located near the inner portion of the disk. Unfortunately, this model is untenable for several reasons: (i) The cloud radius in some cases would need to be $\approx 10^4$ km (Miyamoto, et al., 1991). (ii) There is no plausible energy source so far from the central object. (iii) Electrons cool rather quickly (see Hanawa 1991). (iv) Such a cloud cannot produce the observed

photons of 100 - 500 keV and beyond. (v) The hard and soft radiations are basically uncorrelated (Pan, et al., 1995, Miyamoto, et al., 1988), contrary to expectations if the cloud encloses the soft photon source. (vi) Miyamoto et al. (1988) showed that the time delays of photons passing through such a cloud would be nearly independent of photon energy, contrary to observations for Cyg X-1.

More recent BHC disk models tend toward speculation about the ingredients needed to produce the observed spectral features without relying on a tangible surface. One such model includes non-thermal electron injection, e^+e^- pair production, and soft photon injection (Kusunose, Minishige and Yamada 1996). The difficulties with the model are: (i) How is it possible to get sufficient energy out of the gap? (ii) How are pairs generated and accumulated in the gap, and why should they annihilate in a timely fashion? (iii) How can a cold inner ring and cool photons arise? (iv) How can these features be made strongly mass dependent in order to avoid calculation of excessive hard x-rays for NSBs with their significant surface contributions? (v) Many characteristics, including the size of the cold ring are adjustable parameters.

A recent model devised by Narayan et al. (Narayan, Garcia and McClintock 1997) attempts to provide an explanation of the hard x-ray emissions of the quiescent states of x-ray novae in terms of advective accretion flows in an optically thin disk. The key feature of this type of flow is that the radiative efficiency of the gas is low. High accretion rates are needed to produce quiescent luminosities. The bulk of the viscous dissipation is assumed to be thermalized and advected into the central object. The spectrum of the gas is not the blackbody-like spectrum of the standard (optically thick) thin disk models and the disk luminosity has a quadratic dependence on the accretion rate. If the central object is a neutron star then it is assumed that the advected thermal energy would ultimately reappear as radiation from its surface, although what to do about both quantity and hardness seems to have been overlooked in this model. On the other hand, if the central object is a black hole, the advected energy would vanish. In this model a quiescent advecting black hole is predicted to be as much as 10^4 less luminous than a quiescent neutron star with the same accretion rate. For example, $\approx 10^{-9}$ $M_\odot$/yr is needed to produce a quiescent disk luminosity of $\approx 10^{34}$ erg/s for V404 Cygni. Such an accretion rate for a 1.4 $M_\odot$ neutron star at its 13% (Schwarzschild metric) conversion efficiency would produce 8 x 10^{36} erg/s; which is certainly not a quiescent level for a neutron star. A further difficulty with this model is that by coupling the optically inferred accretion rate to the x-ray production, there is no longer a mechanism for the mass accumulation needed to produce another outburst via disk instability.

Luminosity data from Table 2 of Narayan et al. (1997) for five NSBs and five BHCs is plotted in Figure 5. The lowest point of the plot is for BHC A0620-00. It is about a factor of ten below the Eddington limit for its mass as well as being low at minimum and generally devoid of hard radiations. The first two anomalies could result from an incorrect distance estimate. Its estimated distance is the least of all strong BHCs. If there is a trend of decreasing luminosity for more massive objects, it might be caused by weak propeller effects of the magnetic fields of the objects in the Yilmaz metric model. However, the more likely case, consistent with the data and the Yilmaz model, is that all of these objects have comparable minimum luminosities because they have similar

temperatures and small radiating areas. Figure 5 provides no support whatever for the advection model prediction that quiescent BHCs would be 10^4 lower in luminosity than quiescent NSBs. That they are brighter at maximum only indicates the presence of greater mass and a higher Eddington limit.

It should be clear from the preceding considerations that there is an abundance of evidence for the presence of radiating surfaces in all x-ray novae. Robust models of gap accretion can provide easy explanations of the dominant spectral features. Black hole disk models are incapable of explaining the hardest radiatons of BHCs. They also fail the tests of time resolved spectroscopy and fail in application to NSB disks. The strong implication of this situation is that General Relativity needs modification to eliminate singularities and event hoizons. The Yilmaz theory is attractive because it retains and extends the curved space-time concepts of Einstein. There is a solid research program based on the Yilmaz theory and a potentially seamless chain of calculations on the way to understanding x-ray novae and other gravitationally collapsed objects. Only those who see evidence of event horizons in Figure 5 should see no need to pursue it. As with General Relativity, every test of a theory without adjustable parameters is a potentially fatal test. It is time for serious side-by-side tests of both in this strong field regime.

Acknowledgements

It is a pleasure to acknowledge many stimulating and helpful discussions with my colleagues, Ray C. Jones, Adam Fisher and Charles Rogers. The encouragement of Prof. Carroll O. Alley, University of Maryland, is also appreciated. I am indebted to Adam Fisher for technical assistance.

References

Alley, Carroll O. in Fundamental Problems in Quantum Theory, Annals New York Academy of Sciences 1995, **755**, 464

Balucinska-Church, M., Takahashi, T., Ueda, Y., Church, M., Dotani, T.,Mitsuda,K. and Inoue, H., 1997 ApJ, 480, L115

Barret, D. et al. 1992 ApJ., **394**, 615

Barret, D., McClintock, J., & Grindlay, J., 1996 ApJ, **473**, 1996

Biehle, G. & Blandford, R., 1993 ApJ **411**, 302

Churazov, E., et al., 1995, Apj. **443**, 341

Clapp, R. E., 1973 Phys. Rev. D **7**, 345

Czerny, B., Czerny, M. & Grindlay, J., 1986 ApJ, **311**, 241

Ebisawa, K. et al., 1994 PASJ, **46**, 375

Fortner, B., Lamb, F. & Miller, G., 1989 Nature **342**, 775

Friedman, J. & Ipser J., 1987 ApJ, **314**, 594

Hanawa, T., 1991 ApJ, **373**, 222

Imamura, J., Steiman-Cameron, T. and Middletich, J. 1987 ApJ **314**, L11

Joss, P. & Rappaport, S., 1984, ARA&A, **22**, 546

Kalogera, V. & Baym, G., 1996 ApJ. **470**, L61

Kluzniak, W. & Wilson, J., 1991 ApJ, **372**, L87

Kusunose, M., Minishige, S. & Yamada, T., 1996 ApJ, **457**, 813

Makishima, K. et al., 1986 ApJ **308**, 635

Margon, B., 1984, ARA&A, **22**, 507

Mirabel, I. & Rodriguez, L., 1994 Nature **371**, 46

Miyamoto, S., Kimura, K., & Kitamoto, S., 1991 ApJ **383**, 784

Miyamoto, S., Kitamoto, S., Mitsuda, K., & Dotani, T., 1988 Nature, **336**, 450

Miyamoto, S., Kitamoto, S., Iga, S., Negoro, H. & Terada, K., 1992 ApJ **391**, L21

Narayan, R., Garcia, M., McClintock, J., 1997 ApJ.**478**, L79

Pan, H., Skinner, G., Sunyaev, R. & Borozdin, K., 1995, MNRAS, **274**, L15

Rindler, W. in Essential Relativity, 1969 Van Nostrand Reinhold Co., Canada, p. 146

Sazanov, S., et al. 1994 Astron. Lett., **20**, 787

Singh, K,, Apparao, K. & Kraft, R., 1994 ApJ, **421**, 753

Stella, L., et al. 1985 ApJ, **288**, L45

Sunyaev, R. & Trümper, J., 1979 Nature **279**, 506

Taam, R. & Picklum, R., 1978 ApJ, **224**, 210

Tanaka, Y. & Shibazaki, N., 1996 ARA&A, **34**, 607

Tennant, A., Fabian, A. & Shafer, R., 1986 MNRAS, **221**, 27p

van der Klis, M., 1994 ApJ. **SS92**, 511

Verbunt, F., et al., 1994 A&A, **285**, 903

Walker, M., 1992 ApJ., **385,** 661

White, N. & Marshall, F., 1984 ApJ, **281**, 354

White, N., Stella, L. & Parmar, A., 1988 ApJ, **324**, 363

Yilmaz, H., 1958, Phys. Rev., **111**, 1417

Yilmaz, H., 1971, Phys. Rev. Let., **27**, 1399

Yilmaz, H., 1992, Il Nuovo Cimento, **107B**, 941

Yilmaz H., 1994, in Frontiers of Fundamental Physics, Ed. M. Barone & F. Selleri,

Plenum Press, New York, p. 115
Yilmaz H., 1995, in Fundamental Problems in Quantum Theory, Annals New York Academy of Sciences 1995, **755**, 477

Figure Captions

Fig. 1 Radius, R, gravitational mass, m_g, and surface redshift, z, as functions of free baryon mass, m_b, contained within a neutron star in the exponential metric. Radius is in units of $r_0 = c/\sqrt{4\pi G\rho_0}$ and masses in units of $M_0=c^2r_0/G$. Heavy line features at the lower left are the same quantities for the Schwarzschild metric.

Fig 2. Radius, gravitational mass and surface redshift as functions of free baryon mass for a neutron star in the Schwarzschild metric. Units are the same as Figure 1. Dashed lines show extensions for black holes.

Fig. 3 Efficiencies of conversion of gravitational potential energy to radiation as functions of gravitational mass, m_g. Gravitational mass is in units of M_0. Solid upper lines are $f_s + f_d$. Free baryon mass, m_b, increases from left to right along these curves. The spiral of the Yilmaz metric occurs because maxima and minima of redshift and gravitational mass do not correspond to the same free baryon mass. Lower dotted line is f_d, which is essentially the same in both metrics. Surface radiation is represented by the difference between the upper and lower lines, excepting black holes.

Fig. 4 Binding energy expressed as a fraction of the rest mass-energy of accreted particles; given by (1 - dm_g/dm_b). Collapse of the core in the Schwarzschild metric is shown by the diverging line at the left. The curved line extending to the right is for the Yilmaz metric.

Fig. 5. Log minimum luminosity (erg/s) vs log maximum luminosity for five NSBs and five BHCs. The lowest point is for BHC A0620-00 (see text, see appendix). Data obtained from Narayan et al., (Narayan et al. 1997)

APPENDIX

The mechanics of a particle orbit can be examined very simply with the aid of the energy-momentum four-vector. The magnitude of this vector, given by $g^{ij}p_i p_j$ is $m_0{}^2c^2$ where m_0 is the rest mass of the particle. For a particle in an equatorial orbit ($\theta = \pi$, $p_\theta = 0$) about an object of gravitational mass M in the Schwarzschild metric, one obtains:

$$\frac{E^2}{(\ 1\ -\ 2u\ )c^2}\ -\ (1-2u){p_r}^2\ -\ \frac{{p_\phi}^2}{r^2}\ =\ {m_0}^2c^2 \tag{27}$$

Here $p_0 = E/c$, where E is the particle energy and $uc^2 = GM/r$ is the gravitational potential at distance r from the center of mass M. p_ϕ, the particle angular momentum, is a constant of the motion. Further, by defining $a = (cp_\phi/GMm_0)$ and rearranging, the equation above becomes:

$$(1-2u)^2\frac{{p_r}^2}{{m_0}^2c^2} = \frac{E^2}{{m_0}^2c^4} - (1-2u)(1+a^2u^2) \tag{28}$$

For suitably small energy, bound orbits occur. Turning points for which $p_r = 0$ can be found by examining the effective potential, which consists of all terms to the right of $E^2/{m_0}^2c^4$ above. At minima of the effective potential we find

$$a^2\ =\ \frac{1}{u\ -\ 3u^2} \tag{29}$$

and with $p_r = 0$, we get

$$E\ =\ m_0c^2\frac{(1\ -\ 2u)}{\sqrt{(1\ -\ 3u)}} \tag{30}$$

The innermost marginally stable orbit is found by setting the first two derivatives of the effective potential with respect to u to zero. This gives the well-known results, $u = 1/6$ and $a^2 = 12$. With this value of u, $E = \sqrt{(8/9)}\ m_0c^2$. Substituting this value for E, the radial motion equation for a subsequent geodesic fall to the star surface is:

$$(1\ -2u\ )\frac{{p_r}^2}{{m_0}^2c^2}\ =\ \frac{1}{9}(6u-1)^3 \tag{31}$$

Equating p_r to mv_r, using $m = E/c^2$ and recognizing $(1 - 2u)v_r$ as the proper velocity at the position where the potential is u, the radial velocity relative to a distant observer is seen to be

$$v'_r\ =\ \frac{\sqrt{2}}{4}c(6u-1)^{3/2} \tag{32}$$

Analogous treatment of the orbit equation in the Yilmaz metric yields:

$$\exp(-4u)\frac{{p_r}^2}{{m_0}^2c^2}\ =\ \frac{E^2}{{m_0}^2c^4}\ -\ \exp(-2u)(1\ +\ a^2u^2\exp(-2u)) \tag{33}$$

Setting the first two derivatives of the effective potential to zero in this case produces coupled equations which have a solution for $u = (3 - \sqrt{5})/4 \approx .191$ with a = 12.4. Circular orbits occur for

$$a^2 \;=\; \frac{\exp(2u)}{u \;-\; 2u^2} \tag{34}$$

and

$$E \;=\; m_0 c^2 \exp(-u)\sqrt{\frac{1-u}{1-2u}} \tag{35}$$

A particle in geodesic infall starting with $p_r = 0$ at the marginally stable orbit would arrive at the star with velocity components:

$$v'_r \;=\; c[1 \;-\; 1.12\exp(-2u)(1 \;+\; 12.4u^2 \;\exp(-2u)]^{1/2} \tag{36}$$

$$v'_\phi \;=\; 3.73c\; u \;\exp(-2u) \tag{37}$$

The radial velocity is supersonic for disk temperatures of as much as 1 keV for u = 0.2; i.e., for very little change of potential relative to that of the marginally stable orbit. For u = 0.25, corresponding to the surface of a star of $\approx 3\ M_\odot$, the radial speed for a Keplerian fall from the marginally stable orbit would be about 10^9 cm/s.

In either metric there is an unstable circular photon orbit. In the Yilmaz metric this lies outside the star surface for u(R) > 1/2, or for $m_g > 7\ M_\odot$. For black holes the unstable photon orbit occurs for radius $r = 1.5\ R_s$. Although radially directed photons can always escape in the Yilmaz metric, those with too much orbital angular momentum can be trapped inside the unstable photon orbit. Photon escape is thus hindered by an effective potential barrier. Multiple successful crossings of the barrier could become improbable, thereby impeding the production of hard x-rays by multiple scatterings between the boundary layer and the inner disk. This could occur only for the most massive neutron stars, but could result in their being somewhat dimmed and lacking in hard emissions. It is possible that A0620-00 is an example of such an object.

TABLE 1

Quantities in the Yilmaz Metric

x	f(x)	m_b	m_g	R	z	u(R)	u(0)	gr_0/c^2
0.150	0.993	0.001	0.001	0.148	0.009	0.009	0.013	0.061
0.250	0.980	0.006	0.006	0.148	0.023	0.023	0.033	0.098
0.350	0.961	0.015	0.014	0.242	0.044	0.043	0.063	0.138
0.450	0.936	0.030	0.028	0.328	0.071	0.069	0.102	0.182
0.550	0.907	0.053	0.047	0.406	0.105	0.100	0.149	0.234
∗0.620	0.885	0.074	0.063	0.513	0.131	0.123	0.185	0.272
0.650	0.873	0.085	0.072	0.531	0.145	0.136	0.203	0.293
0.750	0.837	0.124	0.101	0.576	0.191	0.175	0.264	0.361
0.950	0.758	0.229	0.167	0.637	0.299	0.262	0.400	0.534
1.250	0.635	0.441	0.269	0.666	0.497	0.403	0.630	0.906
1.550	0.520	0.697	0.353	0.649	0.724	0.545	0.871	1.45
1.850	0.419	0.974	0.413	0.611	0.966	0.676	1.110	2.18
2.050	0.362	1.160	0.439	0.581	1.130	0.755	1.260	2.76
2.850	0.203	1.830	0.475	0.477	1.710	0.996	1.790	5.65
3.550	0.127	2.290	0.466	0.415	2.070	1.120	2.150	8.29
4.250	0.081	2.590	0.454	0.384	2.260	1.180	2.410	10.1
7.050	0.023	3.330	0.406	0.332	2.390	1.220	3.050	12.5
10.10	0.010	3.700	0.383	0.328	2.220	1.170	3.420	11.5
15.10	0.004	4.050	0.368	0.340	1.950	1.080	3.790	9.40
20.00	0.002	4.270	0.364	0.355	1.780	1.020	4.030	8.00
40.10	0.001	4.800	0.372	0.401	1.530	0.928	4.620	5.85
60.10	0.000	5.130	0.384	0.422	1.490	0.912	4.960	5.38
80.10	0.000	5.390	0.394	0.430	1.500	0.916	5.230	5.31
100.0	0.000	5.600	0.401	0.434	1.520	0.924	5.440	5.39
200.0	0.000	6.290	0.418	0.434	1.620	0.963	6.130	5.81
400.0	0.000	6.980	0.425	0.434	1.670	0.982	6.830	6.04
1000.	0.000	7.900	0.431	0.434	1.700	0.993	7.740	6.17

For x, f(x), see text. R is in units of $r_0 = c/\sqrt{4\pi G\rho_0}$, m_b and m_g in units of $M_0 = c^2 r_0/G$. g is proper surface free-fall acceleration.

$*$ Entries for 1.4 $M_\odot$ with $\rho_0 = 10^{14}$ g/cm^3.

Table 2
Quantities in the Schwarzschild metric.

x	f(x)	m_b	m_g	R	z	u(R)	u(0)	gr_0/c^2
0.143	0.993	0.001	0.001	0.140	0.007	0.007	0.010	0.050
0.288	0.973	0.007	0.007	0.266	0.027	0.026	0.038	0.099
0.498	0.925	0.028	0.026	0.401	0.071	0.062	0.097	0.172
0.653	0.880	0.050	0.044	0.466	0.111	0.095	0.143	0.226
0.803	0.832	0.073	0.061	0.505	0.149	0.122	0.185	0.277
∗0.819	0.826	0.076	0.063	0.507	0.154	0.124	0.190	0.282
0.918	0.793	0.090	0.073	0.524	0.178	0.140	0.214	0.314
1.003	0.765	0.102	0.081	0.534	0.199	0.152	0.234	0.341
1.153	0.716	0.122	0.093	0.545	0.231	0.170	0.264	0.385
1.353	0.655	0.143	0.104	0.550	0.269	0.190	0.297	0.438
1.513	0.609	0.157	0.111	0.550	0.295	0.202	0.318	0.475
1.653	0.573	0.168	0.115	0.549	0.314	0.210	0.334	0.503
1.853	0.526	0.180	0.120	0.546	0.336	0.220	0.353	0.539
2.053	0.484	0.190	0.123	0.542	0.354	0.227	0.368	0.569
2.353	0.430	0.201	0.126	0.536	0.375	0.236	0.386	0.604
2.753	0.373	0.211	0.128	0.529	0.393	0.242	0.404	0.639
3.053	0.338	0.216	0.129	0.524	0.403	0.246	0.414	0.658
3.553	0.291	0.222	0.129	0.518	0.413	0.250	0.427	0.680
4.053	0.255	0.226	0.129	0.514	0.419	0.252	0.437	0.695
4.998	0.206	0.231	0.129	0.508	0.424	0.253	0.449	0.710
6.050	0.168	0.233	0.129	0.504	0.429	0.255	0.458	0.725
8.050	0.125	0.235	0.128	0.501	0.427	0.254	0.469	0.725
10.05	0.100	0.235	0.127	0.500	0.425	0.254	0.475	0.722
15.05	0.066	0.236	0.126	0.500	0.421	0.252	0.483	0.717
20.00	0.050	0.236	0.126	0.500	0.419	0.252	0.488	0.713

For x, f(x), see text. R is in units of $r_0 = c/\sqrt{4\pi G\rho_0}$, m_b and m_g in units of $M_0 = c^2 r_0/G$. g is proper surface free-fall acceleration.
∗ Entries for 1.4 $M_\odot$ with $\rho_0 = 10^{14}$ g/cm^3.

Figure 1

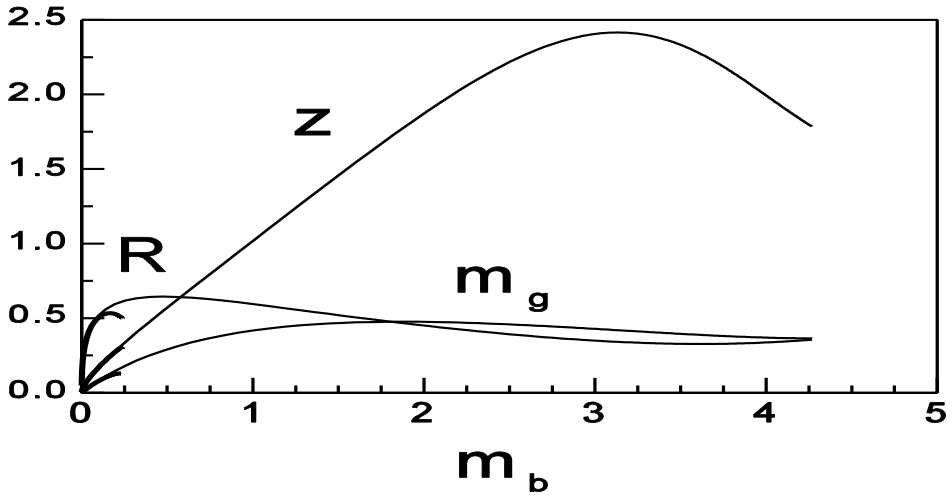

Figure 2

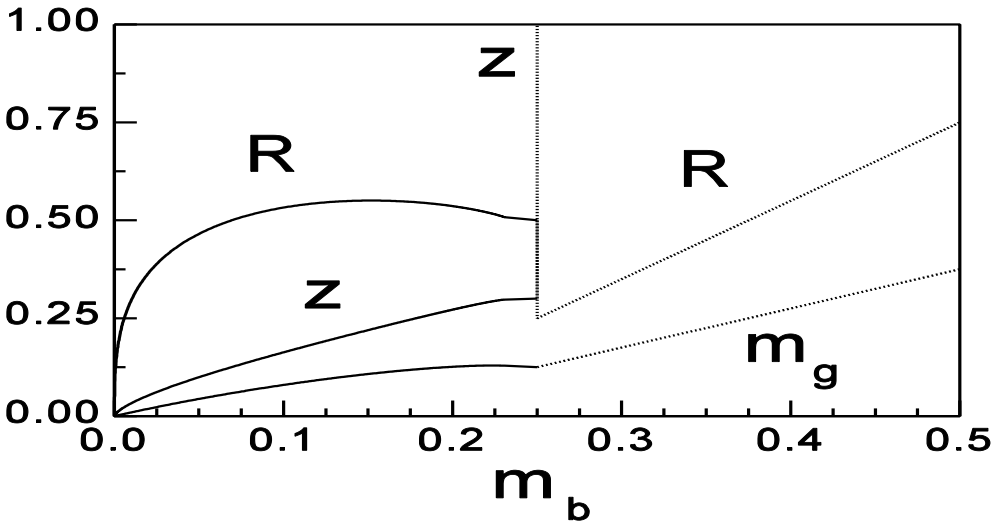

Figure 3

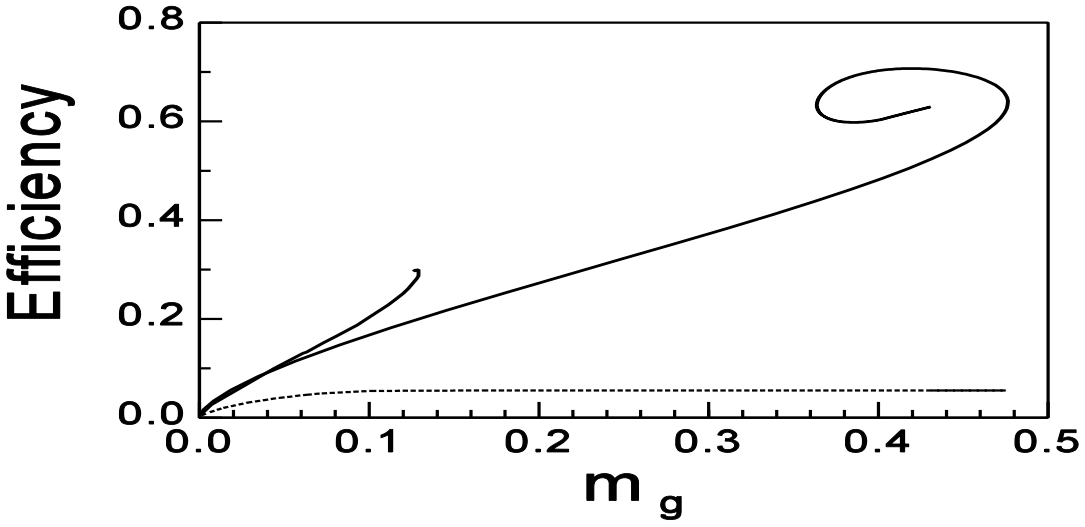

Figure 4

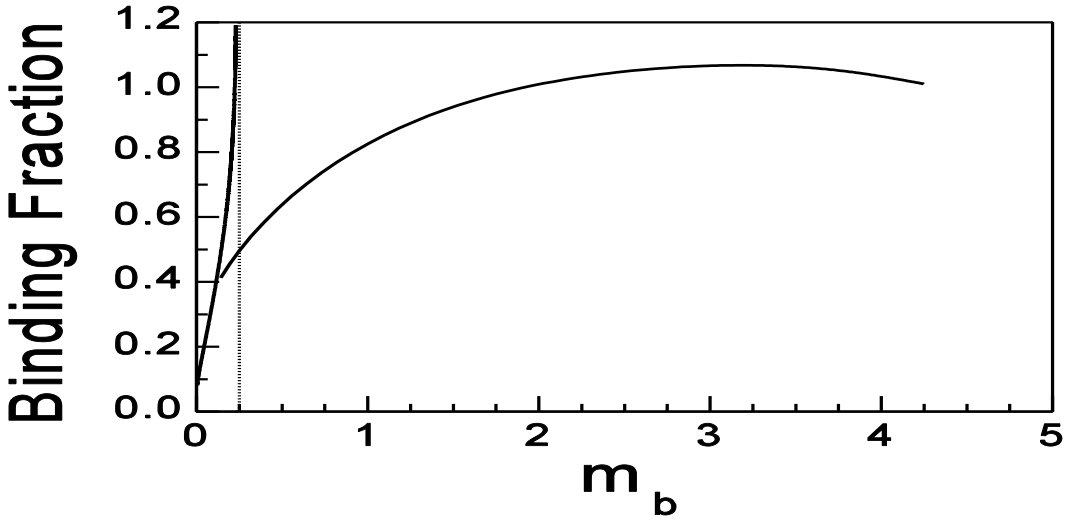

Figure 5